SHMS Lead Glass Calorimeter

Vardan Tadevosyan
Yerevan Physics Institute

April 19, 2002

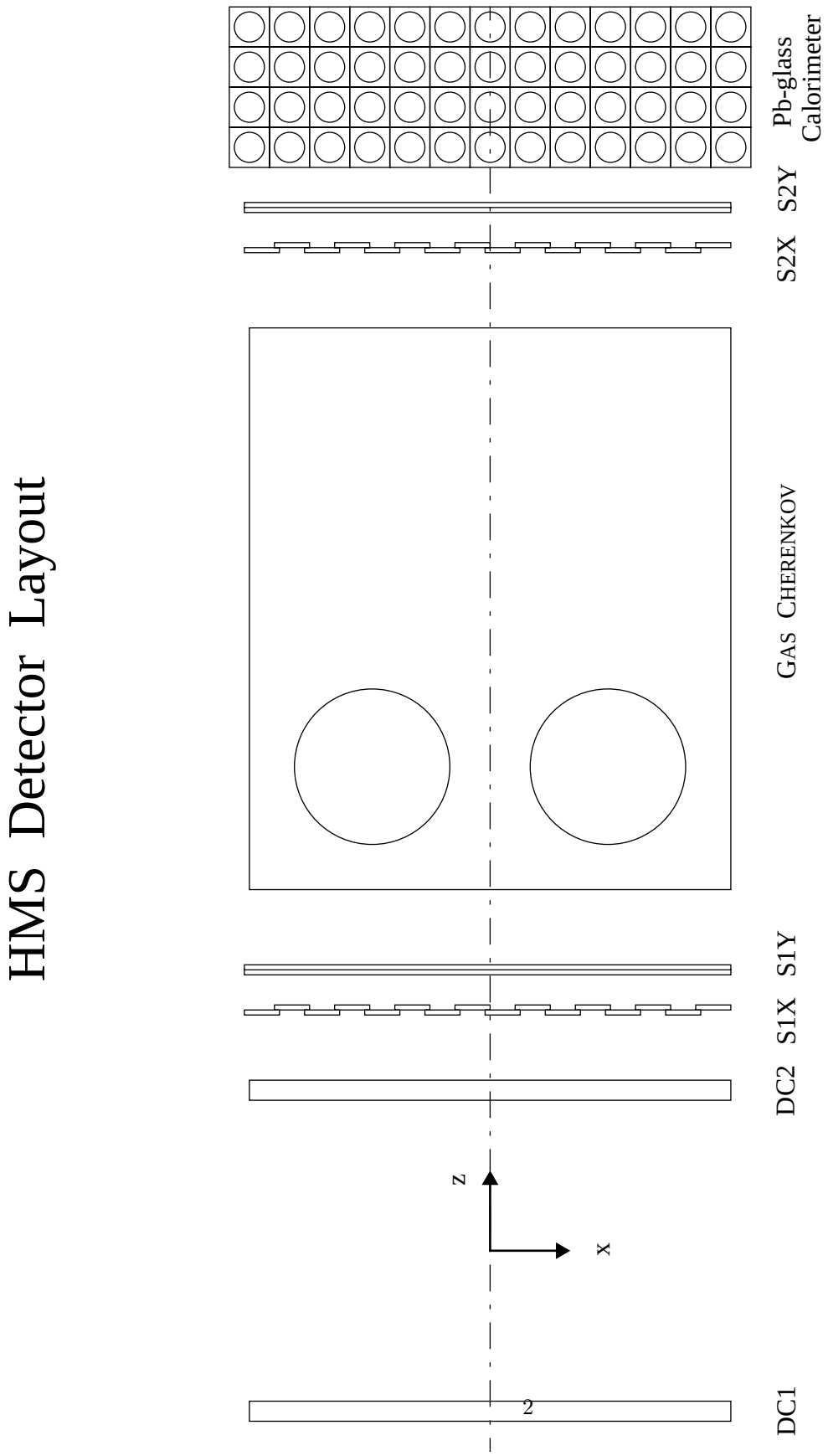

Figure 1: HMS detector package.

Calorimeter Module

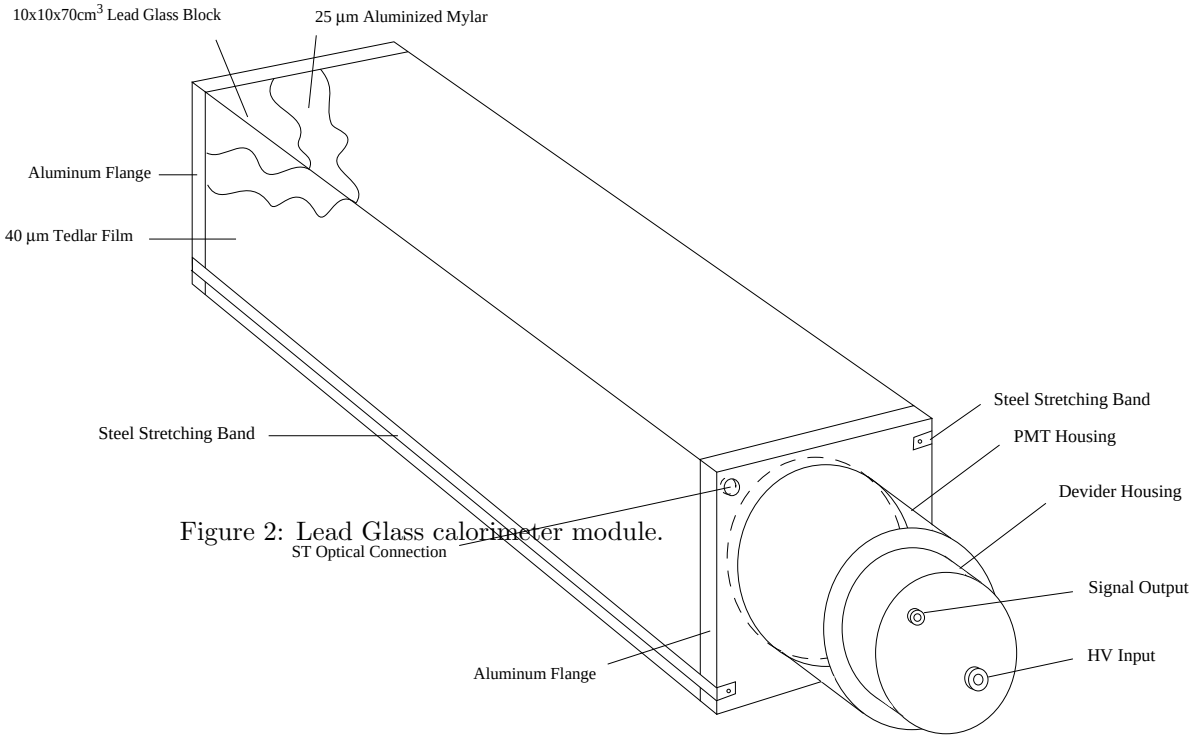

Figure 2: Lead Glass calorimeter module.

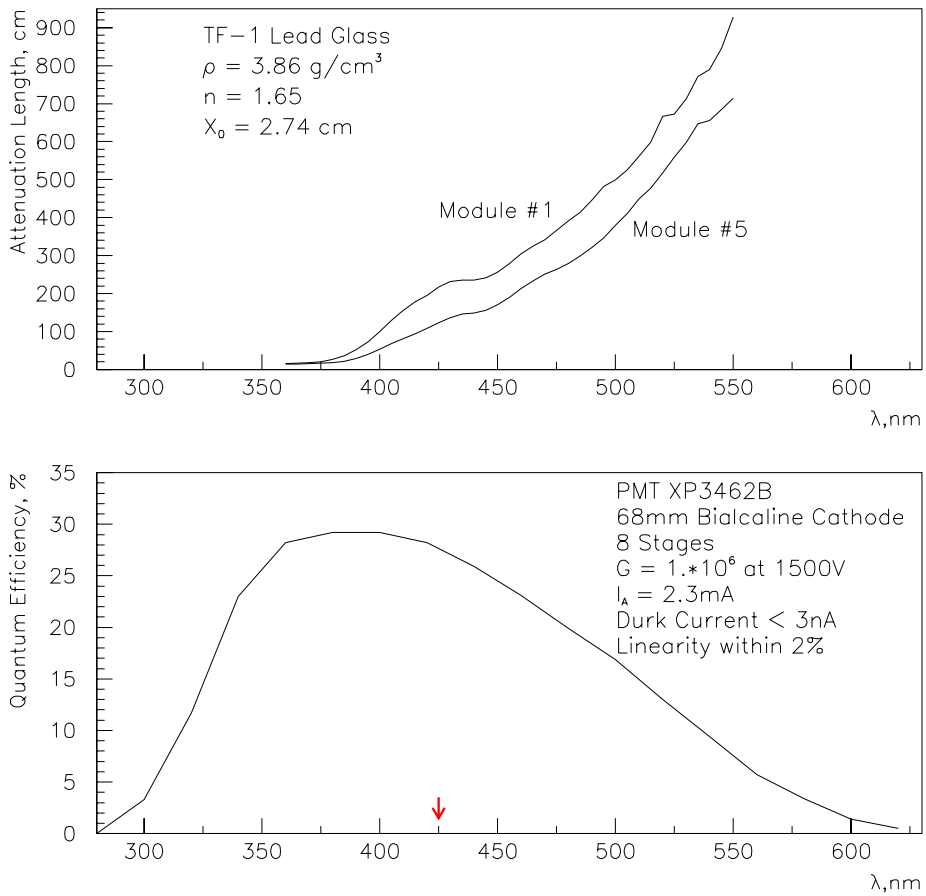

Figure 3: TF-1 Lead Glass attenuation length (top) and Philips PMT XP3462B quantum efficiency (bottom).

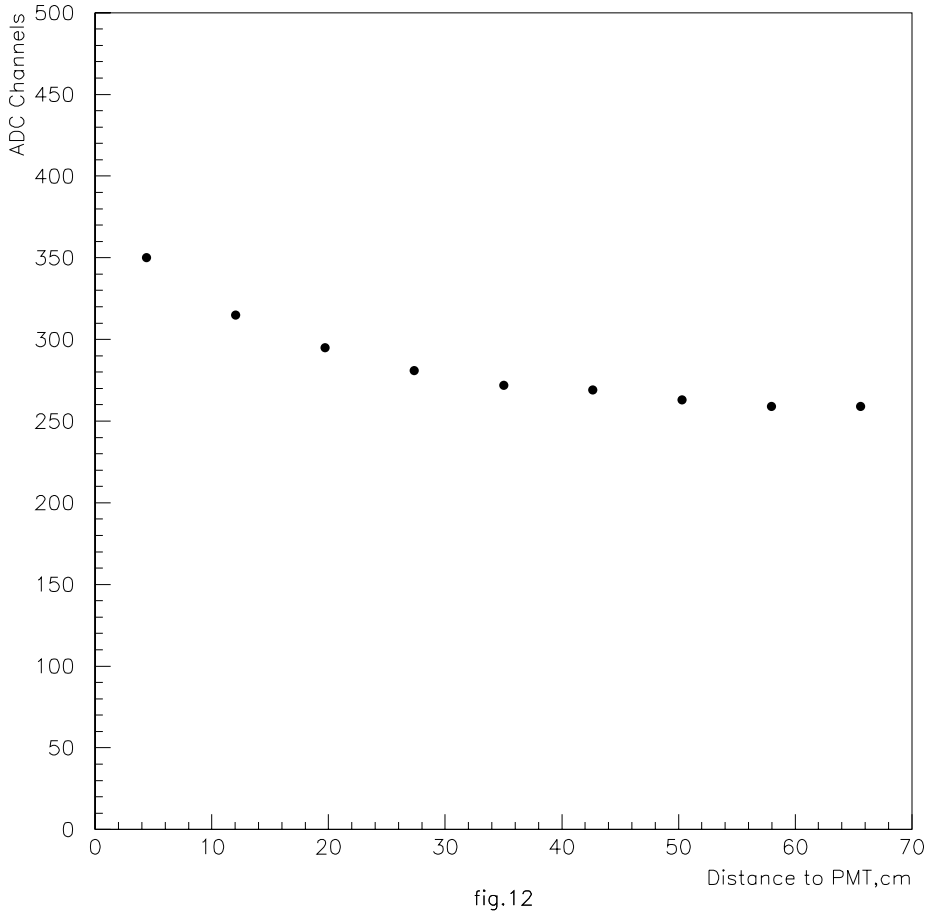

Figure 4: The dependence of PMT responce on the distance to the cosmic ray traversing a Lead Glass module.

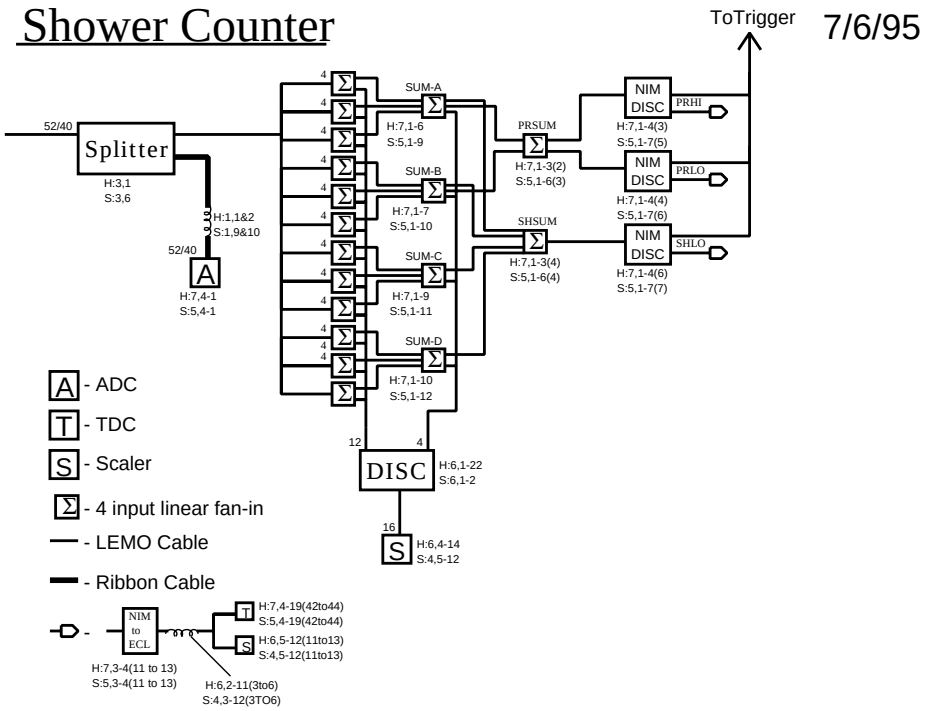

Figure 5: Calorimter part of HMS electronic trigger.

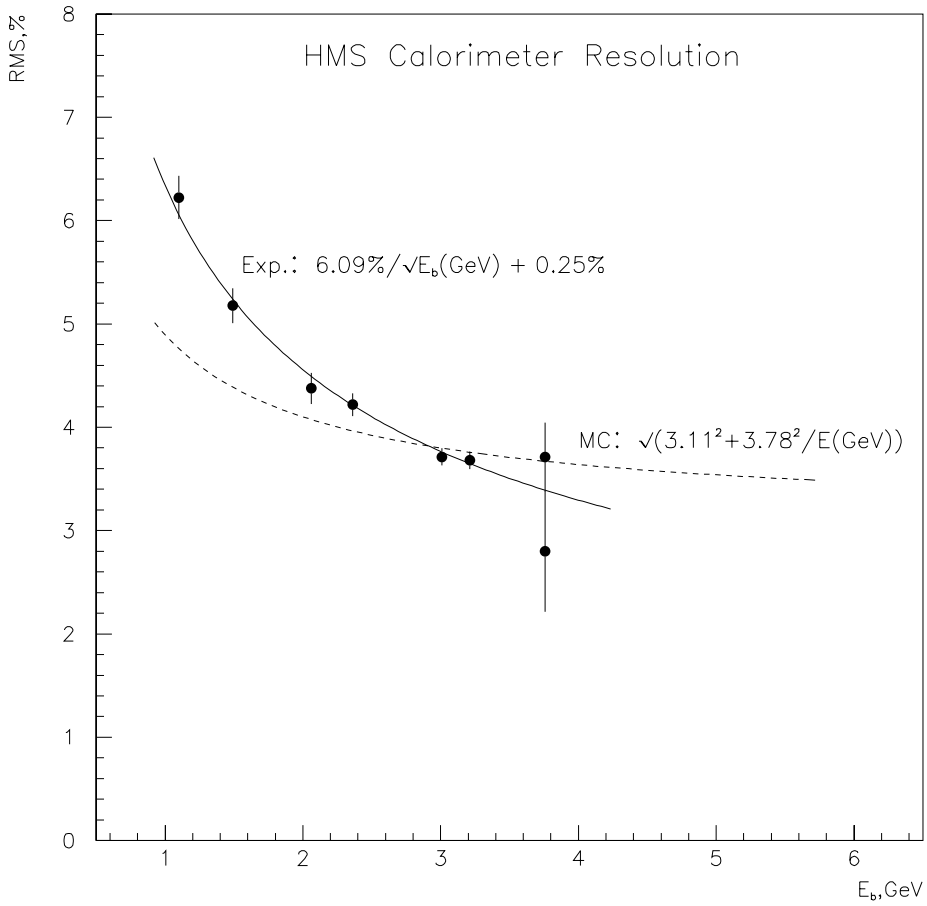

Figure 6: Experimentally measured HMS Calorimeter resolution in comparison with the Monte Carlo simulated.

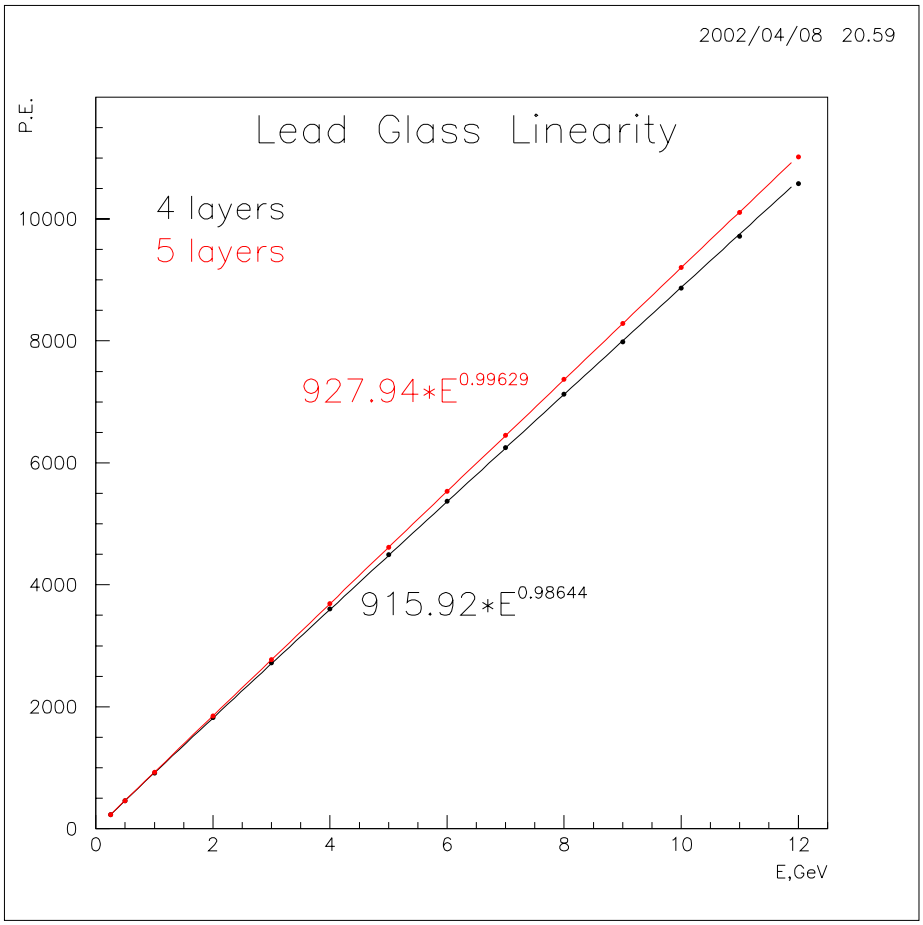

Figure 7: Monte Carlo calculated linearity of Lead Glass calorimeters of 4 and 5 layers.

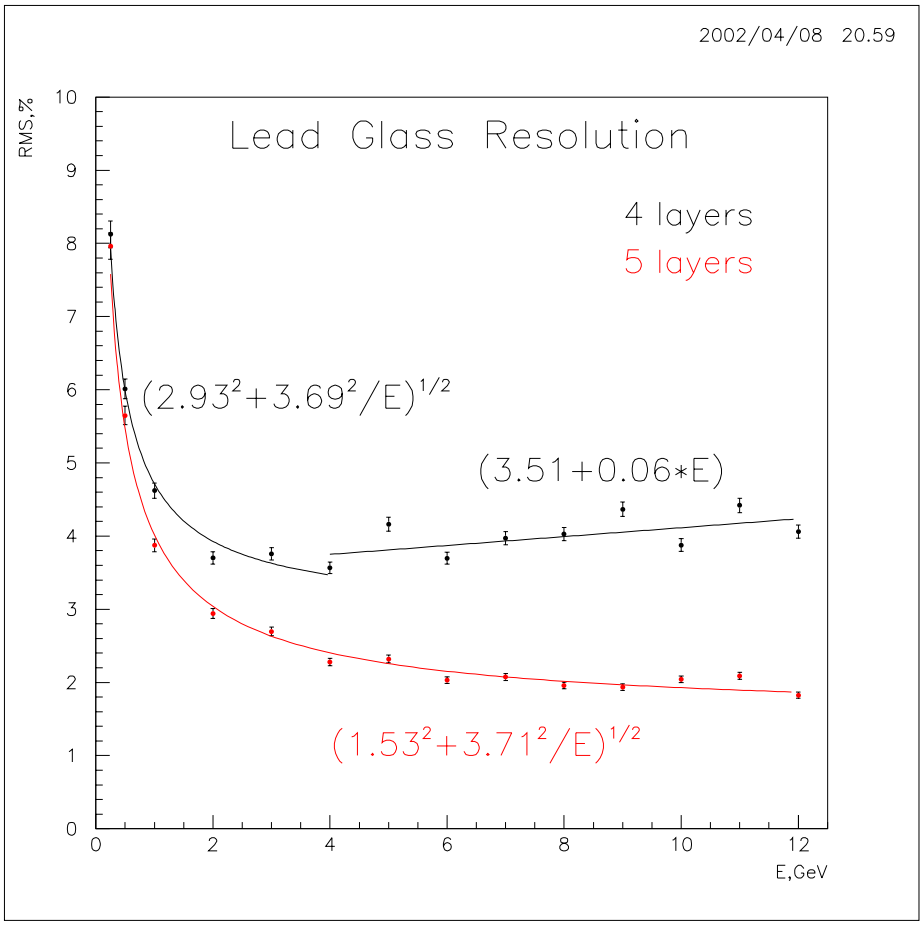

Figure 8: Monte Carlo calculated resolution of Lead Glass calorimeters of 4 and 5 layers.

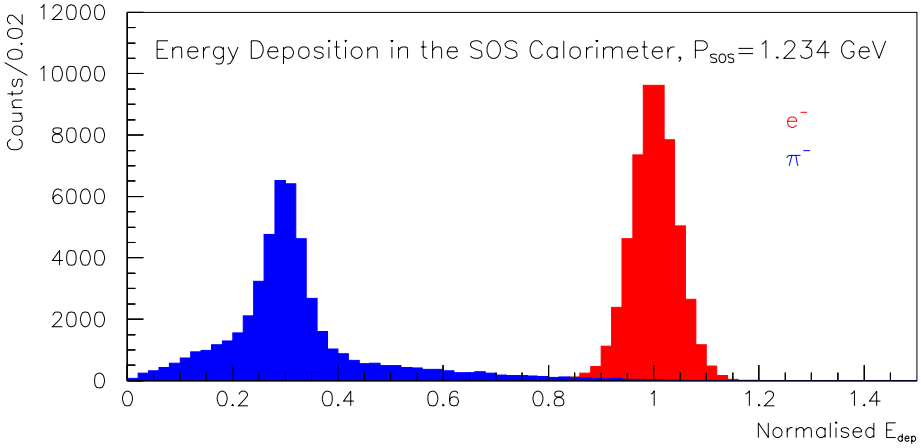

Figure 9: Energy deposition in the SOS calorimeter for the 1.234 GeV/c incident electrons (red) and pions (blue).

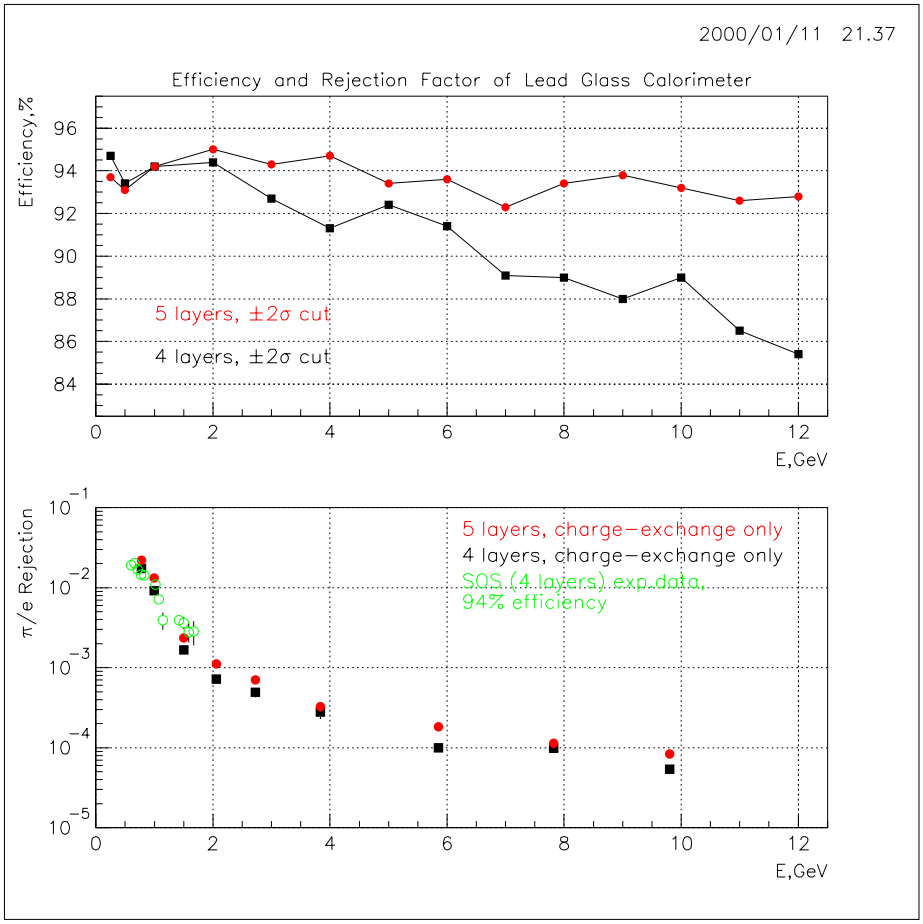

Figure 10: Monte Carlo calculated electron registration efficiency (top) and pion rejection factor (bottom). $\pm 2\sigma$ cut is applyed around electron peak. Only charge exchange reactions are taken into account in pion simulations.

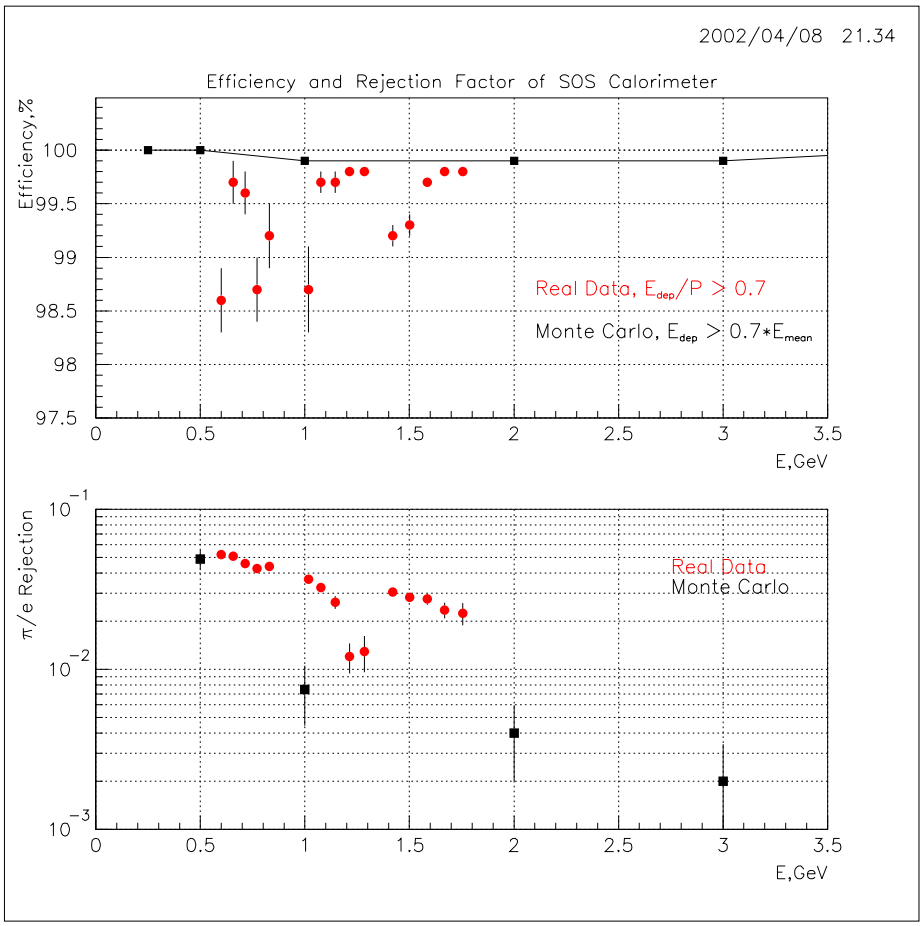

Figure 11: Electron registration efficiency (top) and pion rejection factor (bottom) in 1 GeV/c range, when loose cut $E_{dep}/P > 0.7$ is applyed.

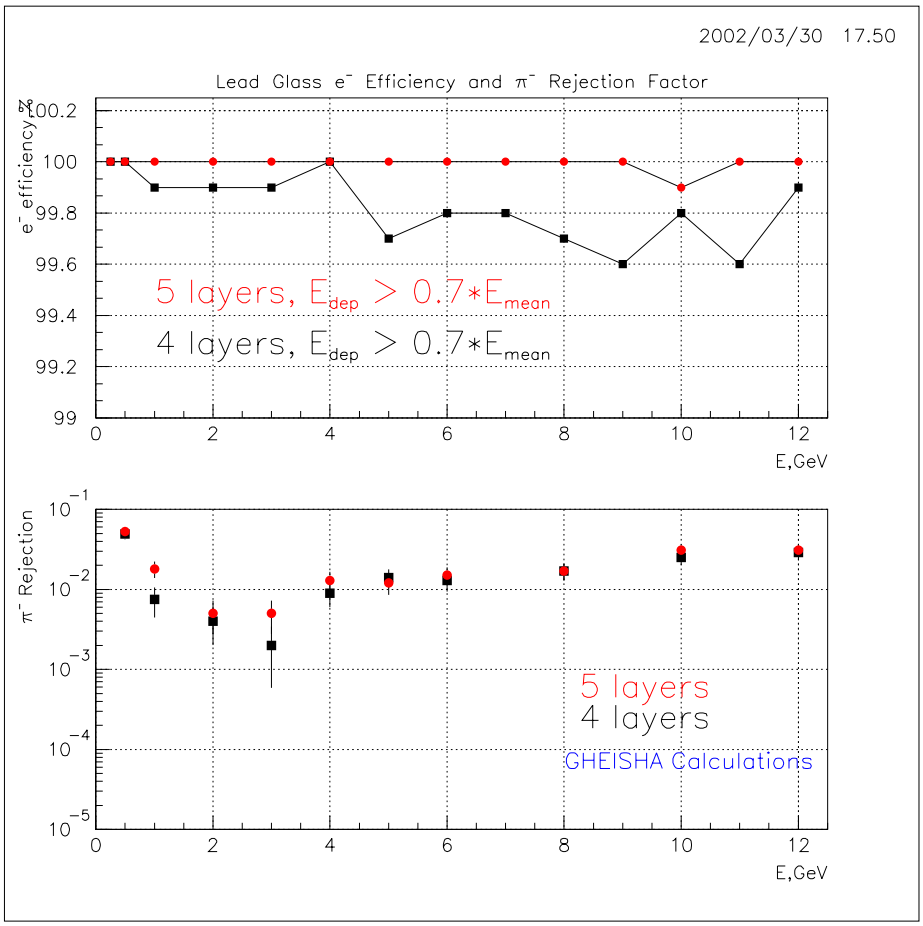

Figure 12: Monte Carlo predictions on electron registration efficiency and pion rejection in up to12 GeV/c range. Loose cut $E_{dep}/P > 0.7$ is applyed.